RADIATION MONITORING SYSTEM USING A PIN PHOTODIODE AT THE KEK ELECTRON/POSITRON INJECTOR LINAC

I. Satake[†,1], H. Iwase[1], T. Suwada[1], S. Kusano[2], D. Asano[3], M. Tokiyoshi[3], Y. Matsumoto[4], Y. Ishigaki[5], M. Sato[6],
[1]High Energy Accelerator Research Organization (KEK), Tsukuba, Japan
[2]Mitsubishi Electric System & Service Co., Ltd, Tokyo, Japan
[3]TAISEI CORPORATION, Tokyo, Japan
[4]Keio University, Yokohama, Japan
[5]The University of Electro-Communications, Chofu, Japan
[6]Yaguchi Electric Corporation, Ishinomaki, Japan

Abstract

We have developed a real-time radiation monitoring system based on a PIN photodiode gamma ray detector. This compact and portable system consists of a small sensor unit and a Raspberry Pi, with control software developed using an EPICS-based framework. The software is designed to support a wide range of radiation measurements. To evaluate the system's measurement accuracy and reproducibility of the system, the sensor was calibrated with Co-60 sources at the KEK radiation irradiation facility. In addition, radiation measurements were conducted during both operation and shutdown of the KEK electron/positron injector LINAC. This paper presents a detailed description of the system and its control software, along with the results of calibration and measurement tests carried out at the facility.

INTRODUCTION

We used a PIN photodiode gamma ray detector (developed by Taisei Corporation, manufactured by Yaguchi Electric Co., Ltd., originally designed by Radiation-Watch Co., Ltd., PocketGeiger (TM) [1]; hereafter referred to as the PIN photodiode sensor) to conduct calibration tests using radiation sources as well as radiation measurements at the KEK electron/positron injector linear accelerator [2] (hereafter referred to as the KEK Linac). The PIN photodiode sensor can be connected to a microcomputer (Raspberry Pi Foundation, trademark Raspberry Pi [3]), enabling real-time radiation monitoring. Furthermore, the system is low-cost, compact, and portable.

The PIN photodiode sensor used in this study is an improved version designed to operate under higher dose-rate environments. The sensor size was reduced to 7.5 × 7.5 mm², less than one-thirteenth of the original, thereby lowering its sensitivity. In calibration tests performed in 2024, the upper measurement limit was approximately 83 μSv/h [4]. In the present study, to further explore the capabilities of the PIN photodiode sensor, we attempted to extend the measurable range by changing the resistor used in the system. Calibration tests were carried out using a Co-60 radiation source, and radiation dose measurements were conducted during both operation and shutdown of the KEK injector Linac. This paper reports the details of these measurement tests in 2025.

† itsuka.satake@kek.jp

SYSTEM CONFIGURATION

The system uses a PIN photodiode sensor as the detector unit, with a Raspberry Pi 4 Model B handling control and data processing. The signal input and output are provided via D-sub connectors, allowing flexible connection between the Raspberry Pi and the sensor. The sensor signal lines from the Raspberry Pi's 40-pin general-purpose input/output (GPIO) header are converted to D-sub connectors. The distance between the Raspberry Pi and the sensor can be adjusted by changing the cable length. Figure 1 shows a photograph of the assembled system with all connections in place.

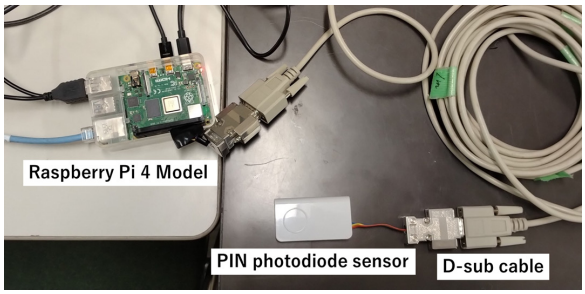

Figure 1: Photograph of the assembled system, showing the PIN photodiode sensor (detector unit) connected to a Raspberry Pi 4 Model B via D-sub cable.

The active area of the PIN photodiode sensor is 7.5 mm². Although the sensor is sensitive to both beta and X/γ rays, a brass plate is placed in front of it to shield beta rays. As a result, the system effectively functions as an X/γ-ray detector in environmental radiation measurements.

SIGNAL ACQUISITION

One PIN photodiode sensor is connected to a single Raspberry Pi, on which an Experimental Physics and Industrial Control System (EPICS) IOC [5] is running. When radiation is detected, the radiation detection signal output is pulled Low through a 10 kΩ pull-up resistor. This signal is acquired via a GPIO pin and the pulses are counted. Within the EPICS IOC, the number of pulses accumulated over one second is calculated and converted into CPS (Counts Per Second) and CPM (Counts Per Minute). The measured CPM is then multiplied by a conversion factor to obtain the dose rate (μSv/h). The information collected by

the EPICS IOC is stored in EPICS PVs and archived through the archiver system. The acquired data items are summarized in Table 1.

Table 1: Acquired Data Items in the Radiation Measurement

Data item	Description
CPM	Counts per minute
Total counts	Total number of counts per day
Dose rate (μSv/h)	Dose rate calculated from CPM
Statistical error	Statistical error of counts N ($\sqrt{N}$)

The waveform of the radiation detection signal observed with an oscilloscope is shown in Fig. 2.

(a)

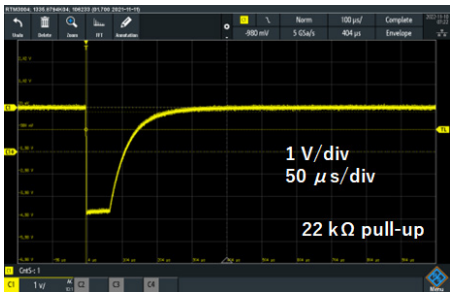

(b)

Figure 2: Radiation detection signal waveforms with different pull-up resistors of (a) 22 kΩ (previous) and (b) 10 kΩ (present).

In the previous system, a 22 kΩ pull-up resistor was used, resulting in a slow rising edge and a distorted waveform. In contrast, the 10 kΩ resistor employed in the present system provides a clear rectangular waveform with a sharp trailing edge.

CALIBRATION

In this study, a Co-60 source with an activity of 98.92 MBq was used. The dose rate was measured by varying the distance between the PIN photodiode sensor and the source from 5 to 50 cm. Measurements were carried out in a large room with a grated metal floor, where the contribution of scattered radiation from walls and floor was considered negligible.

To evaluate the accuracy of the measurement system, the ambient dose equivalent rate constant at 1 cm depth (H*(10)) for Co-60 was applied. Using this constant, the effective dose rate was calculated from the source activity in becquerels (Bq). H*(10) is widely used in radiation protection and is defined as the dose at a depth of 1 cm inside the ICRU sphere (a 30-cm-diameter tissue-equivalent sphere). The ICRU sphere is a conceptual model made of tissue-equivalent material and serves as a reference phantom for dose assessment in radiation protection.

Figure 3 shows the variation in the dose rate as a function of the distance between the PIN photodiode sensor and the source.

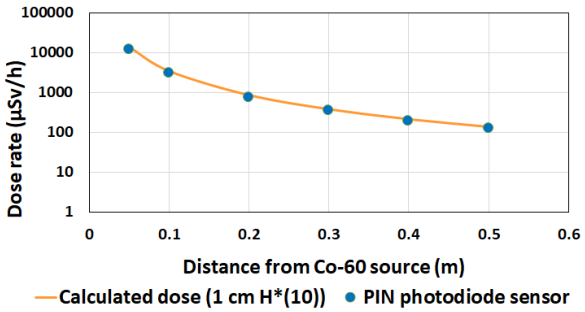

Figure 3: Comparison of the measured dose rates calculated values based on the 1 cm ambient dose equivalent rate constant H*(10) as a function of distance from the Co-60 source.

The experimental results are in good agreement with the calculated values, indicated by the orange line representing the dose rate derived from the 1 cm dose equivalent rate constant. Calibration tests demonstrated consistent agreement with calculated values up to 12.3 mSv/h, confirming the system's measurement capability within this dose rate range. The agreement between the measured and calculated dose rates was quantitatively evaluated using mean absolute error (MAE), mean relative error (MRE), and maximum relative error (MaxRE). MAE represents the average magnitude of absolute errors, while MRE indicates the average relative error in percentage. The evaluation metrics are summarized in Table 2, confirming that the measurement system reproduces the expected dose rates with high accuracy.

Table 2: Evaluation of Co-60 Calibration Dose Rates Using MAE, MRE, and MaxRE

Evaluation metric	Value
MAE (mSv/h)	0.39
MRE (%)	12
MaxRE (%)	14

RADIATION MEASUREMENT

During KEK Linac Operation

During KEK Linac operation, radiation measurements were performed by setting the PIN photodiode sensor and

an Optically Stimulated Luminescence (OSL) dosimeter into the KEK Linac tunnel through an access penetration from the ground level. Measurements were conducted at three locations inside the KEK Linac tunnel, and at each location, the dose rates were recorded at three different heights from the tunnel floor: near the beamline, at mid-height, and near the ceiling. Figure 4 presents the dose rates measured at each location and height inside the tunnel.

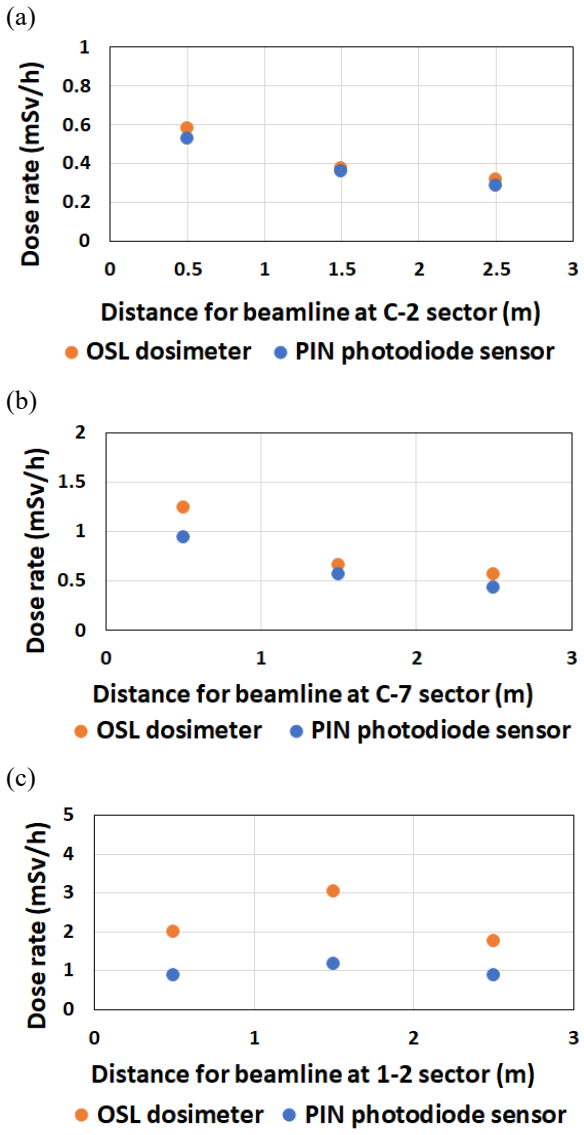

Figure 4: Dose rates measured by the PIN photodiode sensor and the OSL dosimeter at three different locations, (a) C-2, (b) C-7, and (c) 1-2 sectors, and heights in the KEK Linac tunnel during accelerator operation.

Figure 5 shows a schematic layout of the upstream section of the KEK Linac tunnel.

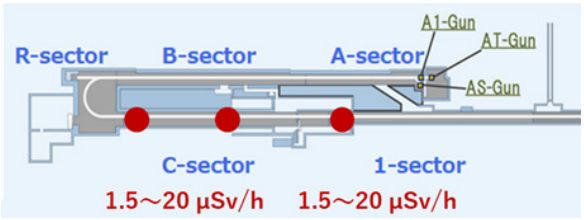

Figure 5: Schematic layout of the upstream section of the KEK Linac tunnel and measurement locations (C-2, C-7, and 1-2 sector).

The KEK Linac is a linear accelerator with a total length of about 700 m, consisting of two straight sections, the A–B sector (~100 m) and the C–5 sector (~600 m), separated by a 180° bending section. Only the upstream section of the tunnel, where the measurements were performed, is shown in this figure. The red marks indicate the measurement locations, where data were taken during accelerator operation. Table 3 presents the evaluation of the PIN photodiode sensor using MAE, MRE, mean error (Bias), and root mean square error (RMSE).

Table 3: Evaluation of PIN Photodiode Sensor using MAE, MRE, Bias, and RMSE

Location (sector)	MAE (mSv/h)	MRE (%)	Bias (mSv/h)	RMSE (mSv/h)
C-2	0.034	7.9	-0.034	0.037
C-7	0.18	21	-0.18	0.20
1-2	1.3	56	-1.3	1.4

Bias indicates the tendency of overestimation or underestimation, and RMSE represents the overall magnitude of error considering its variance. As shown in Fig. 4 and Table 3, the dose rates measured by the PIN photodiode sensor and the OSL dosimeter exhibited sector-dependent trends. In C-2 sector, the dose rates from both devices agreed well, and the associated error metrics were small, indicating high measurement accuracy in the low-dose region. In contrast, larger discrepancies were observed in the relatively high-dose 1-2 sector. In C-7 sector, notable differences appeared near the beamline, whereas measurements at intermediate heights and near the ceiling were well consistent.

These trends are also reflected in the MAE, MRE, Bias, and RMSE values presented in Table 3. The lower error metrics in C-2 sector confirm high agreement between the different sensors, whereas the high-dose 1-2 sector shows increased errors due to larger dose rates. In C-7 sector, Bias and RMSE were larger near the beamline but remained comparatively small at other heights, indicating that the agreement between the different sensors varies with measurement height.

Figure 6 presents the overall dose rate differences across all sectors.

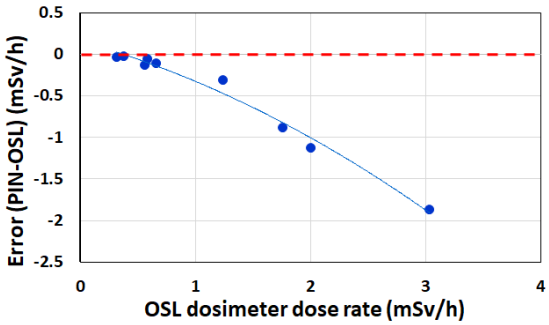

Figure 6: Difference between PIN photodiode sensor and OSL dosimeter dose rates (All sectors combined).

The red dashed line represents perfect agreement between the two sensors, and deviations from this line indicate measurement differences. At lower dose rates less than 0.7 mSv/h, the data are distributed near the red line, whereas at higher dose rates or near the beamline, larger deviations are observed.

These discrepancies at higher dose rates are likely due to count losses in the improved radiation counter. Specifically, the pulsed beam has an extremely short pulse width (~10 ps), which is much shorter than the counter dead time (300 μs), leading to missed counts under these conditions. Additionally, the intrinsic characteristics of the PIN photodiode and the counter's angular dependence may contribute to these differences.

In Fig. 7, corrections with exponential functions were applied either to sector or to dose rate range (low-dose region: <1 mSv/h, high-dose region: ≥1 mSv/h) to examine the agreement between the corrected PIN sensor values and those of the OSL dosimeter.

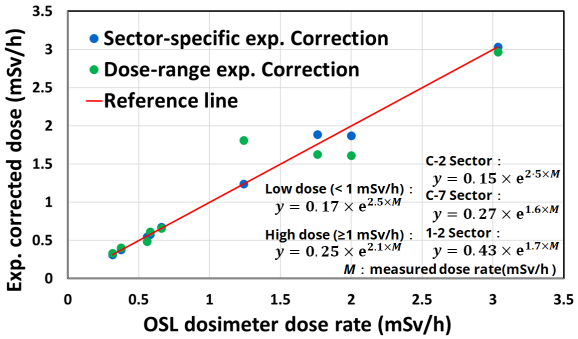

Figure 7: Corrected doses of the PIN photodiode sensor vs. OSL dosimeter dose rates (All sectors combined).

The correction formulae are shown in the figure. After corrections, the PIN sensor values generally agreed more closely with the OSL dosimeter. Comparison indicates that sector-based corrections provided better agreement than the dose-range-based corrections. To quantify the effect of sector-based correction, MAE, MRE, Bias, and RMSE values after corrections are summarized in Table 4 for the C-2, C-7, and 1-2 sectors.

Table 4: Evaluation in the Corrected Doses of the PIN Photodiode Sensor using MAE, MRE, Bias, and RMSE

MAE, MRE, Bias, and RMSE

Location (sector)	MAE (mSv/h)	MRE (%)	Bias (mSv/h)	RMSE (mSv/h)
C-2	0.0030	0.70	0.000	0.0030
C-7	0.0090	1.4	0.000	0.010
1-2	0.085	4.5	0.000	0.10

It shows that the corrections brought the PIN sensor values closer to those of the OSL dosimeter in all sectors.

Discussion on Correction Feasibility

In the present dataset, sector-based corrections were feasible; however, due to variations in radiation levels caused by any beam losses during operation and the lack of measurements at other locations, it cannot be exactly concluded that the dose rates during accelerator operation can be accurately corrected. To assess whether corrections are generally applicable, measurements under some different operational conditions and at different locations are required. Such detailed collection data will allow further verification of the correction method.

After KEK Linac Operation

The PIN photodiode sensor was set into the KEK Linac tunnel to further perform radiation measurements at the transition period from operation to shutdown. Dose rates were measured at three locations inside the tunnel, with the sensor fixed at a height of 1.5 m from the beamline. Figure 8 shows the results on the decay of the dose rates.

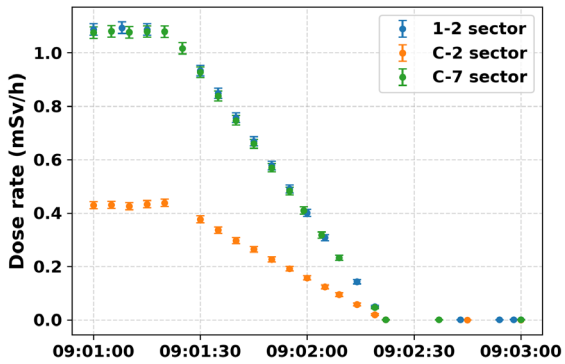

Figure 8: Decay of dose rates measured by the PIN photodiode sensor at the KEK Linac tunnel just after operation stop.

In C-2 sector, the dose rate was approximately 0.4 mSv just after the operation stop, while in C-7 and 1-2 sectors it was about 1 mSv, indicating relatively lower radiation levels. Figure 5 shows the dose rates (in red) measured inside the tunnel after shutdown using a NaI(Tl) scintillation survey meter and a silicon semiconductor survey meter. At three measurement locations, the dose rates were measured to be below 20 μSv with the survey meters. The results are consistent with those by the PIN photodiode sensors.

CONCLUSION

We developed and evaluated an improved realtime radiation monitoring system using a PIN photodiode sensor and Raspberry Pi. Calibration with a Co-60 source confirmed accurate measurements up to 12.3 mSv/h.

Radiation measurements at the KEK Linac showed sector- and height-dependent dose rates, with count losses in high-dose regions due to short beam pulses and counter characteristics. Location-specific corrections generally allowed close agreement with OSL dosimeter readings; however, due to variations in beam losses and the lack of measurements at other locations, additional measurements are required to confirm the applicability of these corrections under different operational conditions.

In low-dose areas, real-time measurements were possible even during operation. The decay patterns of residual radiation in the tunnel depend on beam loss during operation and can vary significantly with each measurement, making real-time measurements during shutdown essential. Such measurements provide an important reference for ensuring a safe working environment.

Future work includes extending measurements to other locations in the KEK Linac and to additional facilities such as the slow-positron facility in KEK. The system is expected to support safe entry decisions during shutdown and contribute to the safety management of personnel and equipment, while efforts will continue to expand its applicability and improve measurement accuracy.

ACKNOWLEDGMENTS

The authors would like to express their sincere gratitude to Mr. Haruo Nagamine, Mr. Kyohei Nishiyama, Mr. Masahiro Taniguchi, and Mr. Tatsuhiko Yoshimoto of the Radiation Team, Project Planning Department, Nuclear Facilities Division, TAISEI CORPORATION, for their invaluable support in the development of the measurement system using an improved PIN photodiode sensor.

REFERENCES

[1] PocketGeiger, http://www.radiation-watch.org

[2] H. Ego *et al*., "Improvement on beam injection by the upgrade of KEK electron/positron injector linac", presented at 22nd Annual Meeting of Particle Accelerator Society of Japan, Tokyo, Japan, Aug. 2025, paper THP004, to be published.

[3] Raspberry Pi, https://www.raspberrypi.com/.

[4] I. Satake *et al*., "Construction of the measurement system using an improved PIN photodiode radiation counter at the KEK electron/positron injector linac", in *Proc. 21st Annual Meeting of Particle Accelerator Society of Japan*, Yamagata, Japan, Aug. 2024, pp. 1022-1025.

[5] EPICS, https://epics-controls.org/.